Biomedical & Pharmacology Journal, December 2022. Vol. **15**(4), p. 2203-2208

Preprocessing of Skin Cancer Images using Non-Local Means (NLM) Filter

M. Reshma[1] and S.H. Ataulla[2]*

[1]Department of ECE, UBDTCE, Davangre, India.
[2]Automation Anywhere, Bangalore, India.
*Corresponding Author E-mail: ataulla@gmail.com

https://dx.doi.org/10.13005/bpj/2557

(Received: 07 April 2022; accepted: 06 September 2022)

The most consecutive malignant growth in the body is skin disease. Every time, more than individualities on the world are determined to have skin malicious growth. The operation of this malice is greatly impressed by early discovery. A new optimum and automatic channel strategy for diagnosing this complaint using dermoscopy images is proposed in this paper. Before processing, the approach comprises a noise reduction process to exclude the disturbances. The BRISQUE score is a quality index that's used to assess different denoising techniques. Filters like anisotropic diffusion and a bilateral are employed for subjective judgment.

Keywords: Anisotropic Diffusion Filter; Bilateral Filter; Blind/'Referenceless' Image Spatial Quality Evaluator; Degree of smoothing; Non Local Means.

Melanoma is known as the everyday most cancers in women and men. There were approximately 300,000 new instances in 2018[1]. Dermascopy is a primary tool for the diagnosis of melanoma. In the dermoscopy images, there is a small amount of noise. During sharpening and contrast improvement, the noise may be enhanced. The additional noise may impair the efficacy of edge-based segmentation algorithms used to extract the borders of skin lesions[2,3]. As a result, denoising is an important step in the automated analysis of dermoscopy images.[4,5]. For denoising of dermoscopy images, the Non-Local Means (NLM) filter is employed. For contrast enhancement, the 'Robust Image Contrast Enhancement (RICE)' method is used[6]. For sharpening, Unsharp Masking is usedA transmittance estimation-based method is used to remove reflections[7]. For virtual shaving, a phase congruency-based approach is applied. The diagrammatic representation of the procedures included in the preprocessing of dermoscopy images is illustrated in Figure. 1.

METHOD

NLM filter

In NLM, for computing the denoised pixel value, the pixel values close to the current pixel within the whole noisy image are taken into account, instead of the pixels geometrically/spatially near to the current pixel[8]. The term 'non-local' in the name of the NLM filter reflects the above concept. For computing, the objective similarity between the current pixel to be denoised and an arbitrary pixel in the input image, a block of pixels around both of them are considered. In denoising techniques[9]

like the bilateral filter, individual pixels are compared instead of comparing the complete block of pixels around the current pixels and the pixel being compared. Consequently, the way of computing the objective similarity is more robust, compared to the way adopted in other denoising techniques like the bilateral filter. The procedure of taking the entire pixels into account for computing each denoised pixel value will increase the time complexity of the NLM filter, uncontrollably. In practice, for estimating the denoised pixel value, only the pixels inside the block of a considerably large radius around the pixel to be denoised are considered[10].

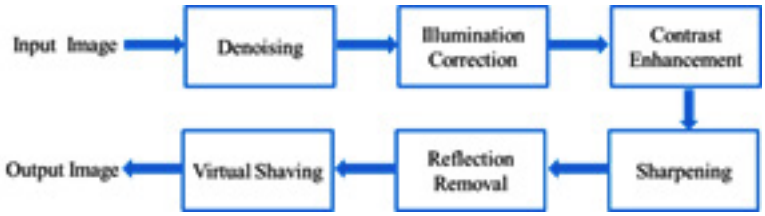

Fig. 1. Schematic of the preprocessing pipeline

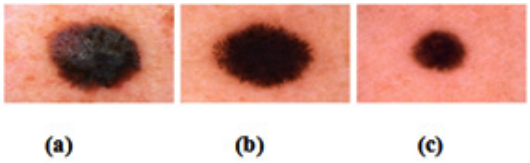

Fig. 2. Representative test images with noise (a) Image1 (b) Image 2 (c) Image 3

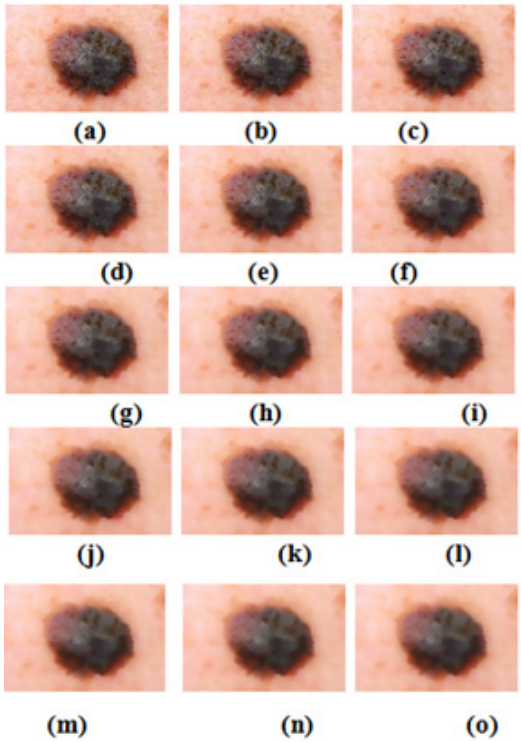

Fig. 3. Output images produced by NLM filter for different values of DoS for test image 1 (a) DoS = 1 (b) DoS = 2 (c) DoS = 3 (d) DoS = 4 (e) DoS = 5 (f) DoS = 6 (g) DoS = 7 (h) DoS = 8 (i) DoS = 9 (j) DoS = 10 (k) DoS = 11 (l) DoS = 12 (m) DoS = 13 (n) DoS = 14 (o) DoS = 15

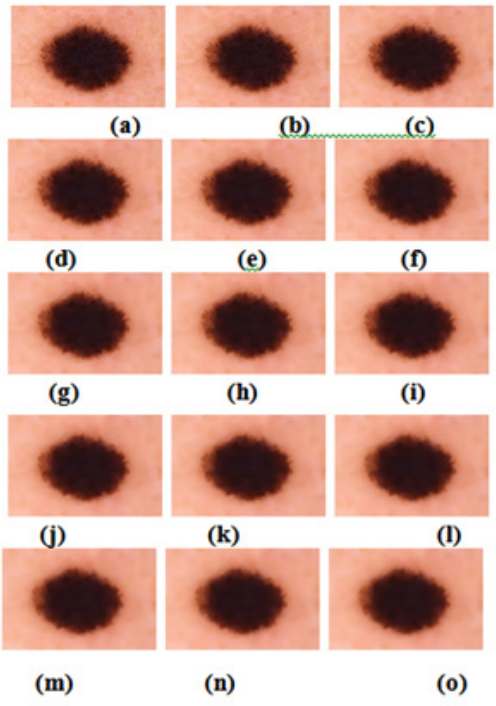

Fig. 4. Output images produced by NLM filter for different values of DoS for test image 2 (a) DoS = 1 (b) DoS = 2 (c) DoS = 3 (d) DoS = 4 (e) DoS = 5 (f) DoS = 6 (g) DoS = 7 (h) DoS = 8 (i) DoS = 9 (j) DoS = 10 (k) DoS = 11 (l) DoS = 12 (m) DoS = 13 (n) DoS = 14 (o) DoS = 15

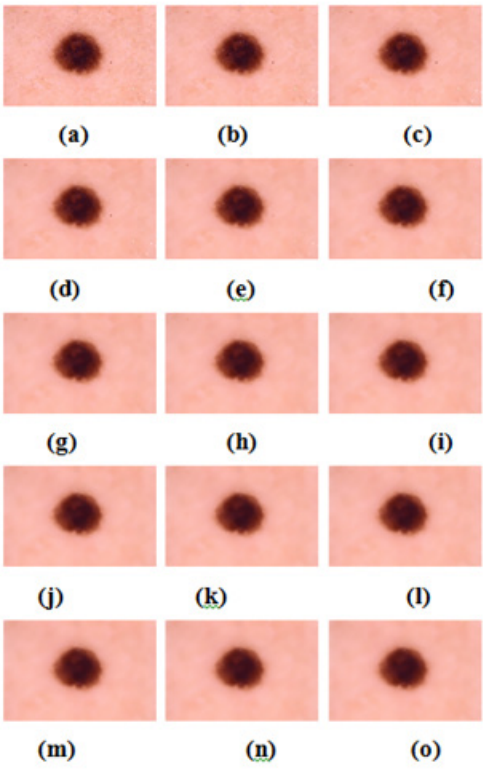

Fig. 5. Output images produced by NLM filter for different values of DoS for test image 3 (a) DoS = 1 (b) DoS = 2 (c) DoS = 3 (d) DoS = 4 (e) DoS = 5 (f) DoS = 6 (g) DoS = 7 (h) DoS = 8 (i) DoS = 9 (j) DoS = 10 (k) DoS = 11 (l) DoS = 12 (m) DoS = 13 (n) DoS = 14 (o) DoS = 15

Objective quality metrics

One objective quality metric is used in this paperthatis Blind/'Referenceless' Image Spatial Quality Evaluator (BRISQUE)[11,12]. BRISQUE score is used to compare different denoising schemes. This quality metric is utilized to objectively determine the value of the degree of smoothing for the NLM filter.

Image dataset

Dermoscopy photos arise from different independent benchmark datasets. The International Skin Imaging Collaboration (ISIC) archive[13] is the first benchmark dataset. The second benchmark dataset is publically available PH2 repository[14]. The ISIC archive comprises a total of 1279 dermoscopy images.

RESULTS AND DISCUSSION

Validation of NLM filter

This section looks at the perceived and objective effects of Degree of Smoothening (DoS) on the NLM filter's denoising quality. The BRISQUE score is used for objective evaluation[15]. Figure 2 illustrates the test photographs. The test images are denoised using the NLM filter with DoS values ranging from 1 to 15, and the results are shown in Figures 3–5.

The smoothing impact on the images grows as the value of the DoS varies from 1 to 15, as seen in Figure. 3 – Figure. 5. For DoS values 1,2 and 3 denoising effect is very less as visible in

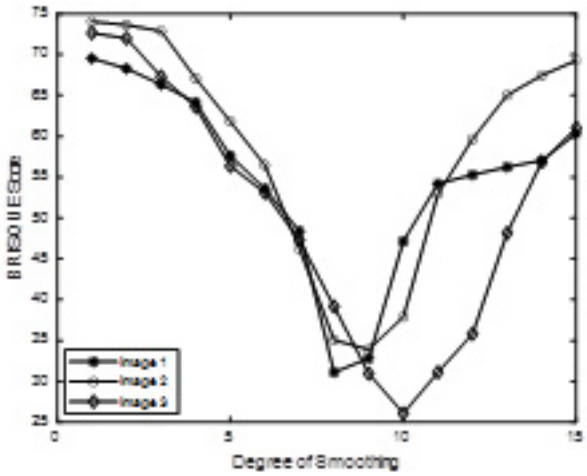

Fig. 6. Variation of BRISQUE score against DoS

Figure. 3(a) - Figure. (c), Figure. 4(a) - Figure.4(c) and Figure.5(a) - Figure.5(c). Smoothening is more effective when DoS values increase beyond 3 as evident inFigure.3(d) - Figure. 3(o), Figure.4(d) - Figure. 4(o) and Figure.5(d) - Figure. 5(o).When the DoS value exceeds 10, however, images become excessively smoothed. This weakens the lesions present in the images as observed in Figure. 3(j) - Figure.3(o), Figure.4(j) - Figure.4(o) and Figure.5(j) - Figure.5(o).As a result, the range of Degree Of Smoothening (DoS) between 6 and 9 is reported to be suitable for dermoscopy images based on the perceived quality of processed images.

For objective evaluation of the quality of images smoothed by NLM, the variations of BRISQUE for various values of DoS is plotted and depicted in Figure.6.The minimum value of the BRISQUE score is appreciable for good quality images[16,17]. The value of BRISQUE decreases as DoS increases from 1 to 8.When DoS is between 8 and 10, BRISQUE has low scores, as shown in the graph. As the DoS rises above 10, the BRIQUE score for all three images increase as well.

This is in agreement with the inferences drawn by inspecting the perceived quality of the resulting images (Figure.3 - Figure.5) for various values of DoS.The NLM filter is compared qualitatively and quantitatively to two other denoising options, namely the anisotropic diffusion filter[18] and the bilateral filter[19]. Output images of the above said algorithms for three input images are illustrated in Figure. 7 to Figure.9.An ideal denoising technique should smoothen the background without fading the boundary of the

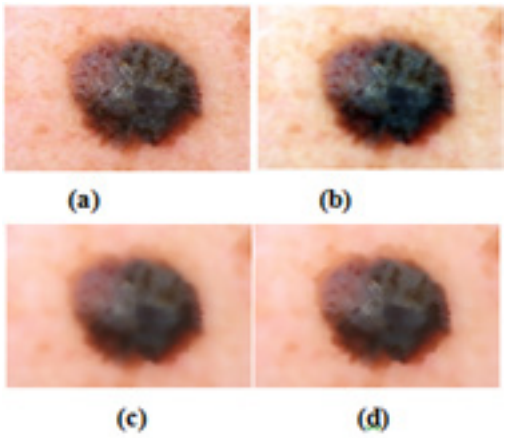

Fig. 7. Output images produced by different denoising algorithms for test image 1 (a) test image 1 (b) anisotropic diffusion filter (c) bilateral filter (d) NLM

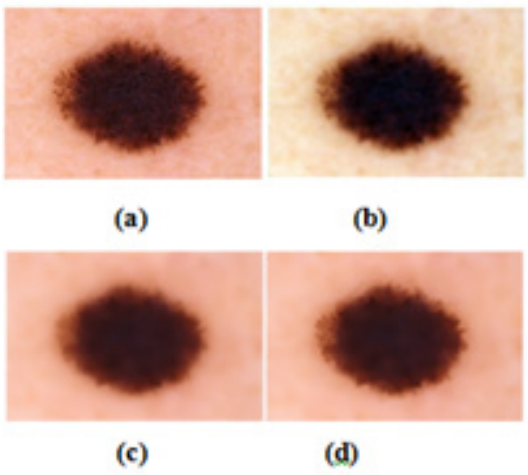

Fig. 8. Output images produced by different denoising algorithms for test image 2 (a) test image 2 (b) anisotropic diffusion filter (c) bilateral filter (d) NLM

Table 1. BRISQUE scores shown by various denoising algorithms

Method	BRISQUE scores
Anisotropic diffusion filter	52.9745±2.9132
Bilateral filter	41.9123±4.1011
NLM filter	34.1123±2.1256

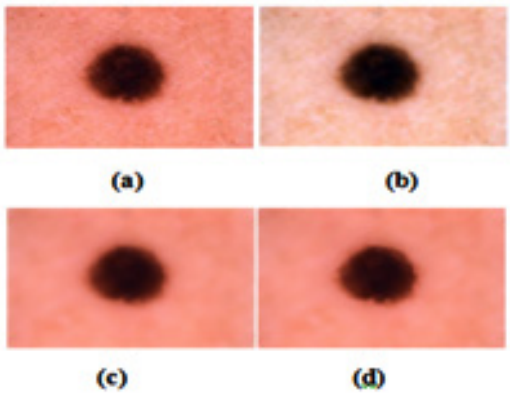

Fig. 9. Output images produced by different denoising algorithms for test image 3 (a) test image3 (b) anisotropic diffusion filter (c) bilateral filter (d) NLM

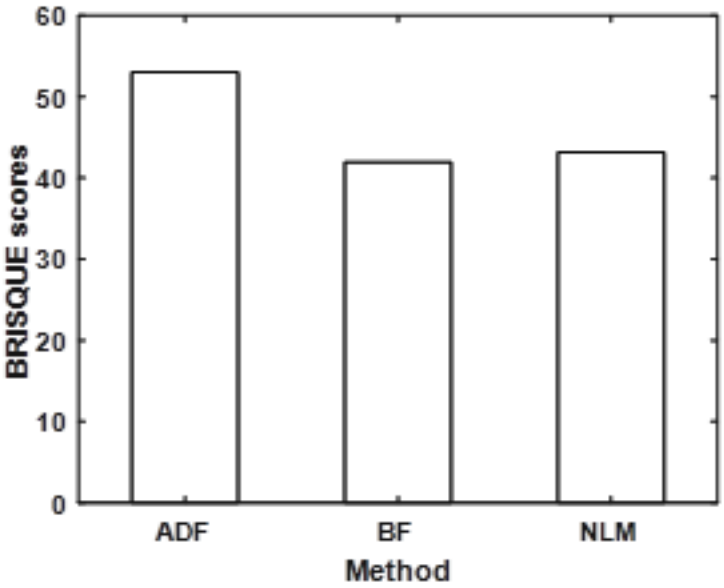

Fig. 10. Bar graph of the BRISQUE scores shown by NLM filter, anisotropy diffusion filter and Bilateral filter on 1279 test images

lesions. Bilateral filter (Figure. 7 (c), Figure. 8 (c) and Figure. 9 (c)) excessively smooths the image. The clarity of the denoised image is considerably reduced as a result, and the lesions' borders fade. The images denoised by anisotropic diffusion filter are illustrated in Figure. 7(b), fig .8 (b) and Figure.9(b).The lesions' boundaries are not well retained in these images.The textural artifact is also visible in the background of the denoised images.The output images of the NLM filter are displayedin

Figure. 7(d), Figure. 8(d) and Figure.9(d). The NLM filter is better than the anisotropic diffusion filter in denoising the image while maintaining the lesions' boundaries.

Information loss is also minimal when compared to bilateral filter. In subjective evaluation, the images denoised by NLM seem to be equally good in smoothing and maintaining the boundary of the lesions than anisotropic diffusion filter and bilateral filter

The BRISQUE scores obtained for anisotropic diffusion filter, bilateral filter and NLM for 1279 images are given in Table 1. The bar graph of the BRISQUE scores is shown in Figure.10. Table 1 shows that the NLM filter produces the lowest value of BRISQUE when compared to other techniques. This supports the inferences drawn from the subjective quality evaluation of the images denoised by different schemes.

CONCLUSIONS

The preprocessing of dermoscopy pictures is acted in this paper. The initial step of preprocessing is denoising. The Non-Local Means (NLM) channel is applied for denoising of dermoscopy pictures. NLM channel displays the most minimal Blind/'Referenceless' Image Spatial Quality Evaluator (BRISQUE) score, contrasted with other denoising plans like anisotropic dissemination channel and respective channel. The result pictures delivered by the NLM channel have insignificant commotion contrasted with that of the bilateral filter and anisotropic diffusion filter.

REFERENCES

1. C. Mattiuzzi and G. Lippi,(2020) "Cancer statistics: a comparison between world health organization (WHO) and global burden of disease (GBD)," *European Journal of Public Health*, **30**(5): 1026-1027.
2. Kuppusamy. P.G, et al., (2019), "A Customized Nonlocal Restoration Scheme with Adaptive

Strength of Smoothening for MR images", *Biomedical Signal Processing and Control,* **49**: 160-172.

3. R. Navid, A. Mohsen, K. Maryam et al.,(2020) "Computer-aided diagnosis of skin cancer: a review," *Current Medical Imaging*, **16**(7): 781–793.
4. Bayraktar. M (2019), "Local Edge-Enhanced Active Contour for Accurate Skin Lesion Border Detection", *BMC Bioinformatics,* **20**(91): 87-97
5. Z. Xu, F. R. Sheykhahmad, N. Ghadimi, and R. Navid(2020), "Computer-aided diagnosis of skin cancer based on soft computing techniques," *Open Medicine*, **15**(1): 860–871. 2020.
6. Fan. X (2020), "Effect of image noise on the classification of skin lesions using deep convolutional neural networks", *Tsinghua Science and Technology,* **25**(3): 425-434.
7. Hegde. P.R, Shenoy. M.M, and Shekar. B.H (2017), "Noise Removal in Dermoscopic Images Using a Novel Software". *Indian dermatology online journal,* **8**(6): 513.
8. Huang. S (2013), "Efficient Contrast Enhancement using Adaptive Gamma Correction with Weighting Distribution", *IEEE Transactions on Image Processing,* **22**(3): 1032-1041
9. Garnavi. R (2012), "Computer-Aided Diagnosis of Melanoma Using Border and Wavelet-Based Texture Analysis", *IEEE Transactions on Information Technology in Biomedicine,* **16**(6): 1239-1252.
10. J. Salmon, R. Willett, and E. Arias-Castro,(2012) "A two-stage denoising filter: the preprocessed Yaroslavsky filter," in *2012 IEEE Statistical Signal Processing Workshop (SSP)*, pp. 464–467, Ann Arbor, MI, USA. 2012.
11. Mittal. A (2012), "No-Reference Image Quality Assessment in the Spatial Domain", *IEEE Transactions on Image Processing,* **21**(12): 4695-4708.
12. Horé. A and Ziou. D (2010), "Image Quality Metrics: PSNR Vs. SSIM", 20th International Conference, Pattern Recognition, Istanbul, Turkey, pp. 2366-2369
13. Gutman. D (2016), "Skin Lesion Analysis Toward Melanoma Detection: A Challenge at the 2017 International Symposium on Biomedical Imaging (ISBI), Hosted by the International Skin Imaging Collaboration (ISIC)", IEEE 15th International Symposium Biomedical Imaging (ISBI 2018), Washington, DC, pp. 168-172.
14. Mendonça. T, et al. (2013), "PH 2 - A dermoscopic image database for research and benchmarking", Proc. 35th annual international conference of the IEEE engineering in medicine and biology society (EMBC), pp. 5437-5440, IEEE
15. N. Razmjooy, V. V. Estrela, and H. J. Loschi, (2020) "Entropy-based breast cancer detection in digital mammograms using world cup optimizationalgorithm," *International Journal of Swarm Intelligence Research (IJSIR)*, **11**(3): 1–18. 2020.
16. Y. Sugiarti, J. Na'am, D. Indra, and J. Santony, (2019) "An artificial neural network approach for detecting skin cancer," *TELKOMNIKA Telecommunication Computing Electronics and Control*, **17**(2): 788–793. 2019.
17. Arici. T (2009), "A Histogram Modification Framework and Its Application for Image Contrast Enhancement", *IEEE Transactions on Image Processing,* **18**(9): 1921-1935.
18. Mishra. D (2018), "Edge Probability and Pixel Relativity-Based Speckle Reducing Anisotropic Diffusion", *IEEE Transactions on Image Processing,* **27**(2): 649-664.
19. Gavaskar. R.G and Chaudhury. K.N (2019), "Fast Adaptive Bilateral Filtering", *IEEE Transactions on Image Processing,* **28**(2): 779-790